IEEE Access
Multidisciplinary | Rapid Review | Open Access Journal

Received September 15, 2019, accepted September 28, 2019, date of publication October 3, 2019,
date of current version October 17, 2019.

Digital Object Identifier 10.1109/ACCESS.2019.2945484

Encoding Multiple Sensor Data for Robotic Learning Skills From Multimodal Demonstration

CHAO ZENG[1,4], (Student Member, IEEE), CHENGUANG YANG[2], (Senior Member, IEEE), JUNPEI ZHONG[3], AND JIANWEI ZHANG[4], (Member, IEEE)

[1]School of Automation Science and Engineering, South China University of Technology, Guangzhou 510641, China
[2]Bristol Robotics Laboratory, University of the West of England, Bristol BS16 1QY, U.K.
[3]School of Science and Technology, Nottingham Trent University, Nottingham NG11 8NS, U.K.
[4]TAMS Group, Informatics, University of Hamburg, D22527 Hamburg, Germany

Corresponding author: Chenguang Yang (cyang@ieee.org)

This work was supported in part by the Engineering and Physical Sciences Research Council (EPSRC) under Grant EP/S001913.

ABSTRACT Learning a task such as pushing something, where the constraints of both position and force have to be satisfied, is usually difficult for a collaborative robot. In this work, we propose a multimodal teaching-by-demonstration system which can enable the robot to perform this kind of tasks. The basic idea is to transfer the adaptation of multi-modal information from a human tutor to the robot by taking account of multiple sensor signals (i.e., motion trajectories, stiffness, and force profiles). The human tutor's stiffness is estimated based on the limb surface electromyography (EMG) signals obtained from the demonstration phase. The force profiles in Cartesian space are collected from a force/torque sensor mounted between the robot endpoint and the tool. Subsequently, the hidden semi-Markov model (HSMM) is used to encode the multiple signals in a unified manner. The correlations between position and the other three control variables (i.e., velocity, stiffness and force) are encoded with separate HSMM models. Based on the estimated parameters of the HSMM model, the Gaussian mixture regression (GMR) is then utilized to generate the expected control variables. The learned variables are further mapped into an impedance controller in the joint space through inverse kinematics for the reproduction of the task. Comparative tests have been conducted to verify the effectiveness of our approach on a Baxter robot.

INDEX TERMS Robotic control, stiffness and force adaptation, multimodal learning, physical human-robot interaction.

I. INTRODUCTION

Robots are increasingly expected to become intelligent enough to automatically adapt to future industrial application scenarios, where small batch production, personalized demand and short cycle are the basic requirements that need to be well satisfied [1]. Unfortunately, due to a number of problems nowadays' robots are far beyond of this expectation. One of the core problems behind this is how to enable a robot to efficiently learn a skill when dealing with a specific task [2], [3]. Traditional robotic programming techniques are often time consuming, low efficiency and high labor cost, making it not suitable for the usage for the learning of robotic skills. One possible and promising way is to transfer skills to the robots by using machine learning and artificial intelligence approaches, which has recently attracted much attention in the field of robotics. For example, robots could be enabled to learn skills from humans, other real-world/simulated robots, or even by watching videos [4], etc.

Among these approaches, teaching-by-demonstration (TbD) is considered as an effective and efficient way for robots to directly learn skills from humans [5], [6]. In a typical TbD system, the robot can imitate the human tutor's behaviour/action after the human tutor demonstrates how to perform a task, which is quite different from the traditional ways. One great advantage of TbD is that an expert (e.g., a mechanical engineer or a software developer) is no longer strongly demanded in a production line for the programming

The associate editor coordinating the review of this manuscript and approving it for publication was Aysegul Ucar.

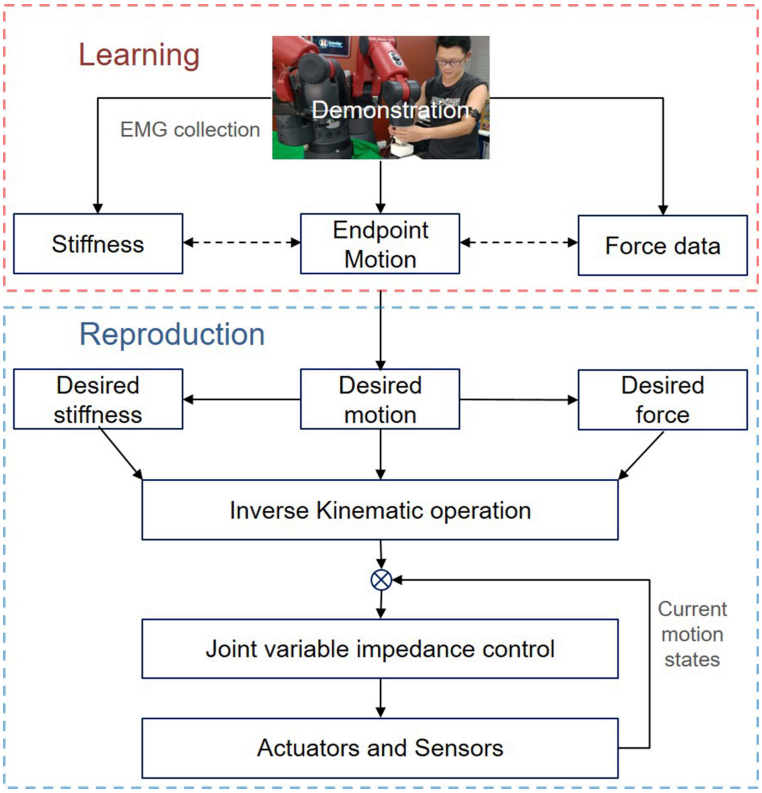

FIGURE 1. The overview of the proposed approach. It consists of a two-phase learning-reproduction architecture: in the learning phase, multimodal sensor signals collected from human demonstration are encoded, in order to learn control variables that can account for a specific task. In the reproduction phase, the robot is then required to perform the task based on the learned multimodal control variables.

of the robot since TbD can low technical barriers and an ordinary worker could efficiently program the robot through demonstration [7], [8].

In order to facilitate human-robot interaction and collaboration, a number of light-weight robotic platforms (e.g., Baxter and Sawyer from Rethink Robotics) have been very recently developed. These robots are designed and manufactured with the purpose that humans can directly and friendly interact or collaborate with the robots. The output forces/torques are usually restricted into a proper range for the concern of safety. However, it is strange to find that to perform a task which looks like a easy one (e.g., pushing a button) seems sometimes not easy at all for a light-weight robot (e.g., Baxter). This may be due to the limited output forces, but more importantly the lack of adaptability which is, however, necessary for the tasks that require the consideration of force/stiffness constraints [9], [10]. This paper aims to provide a promising TbD solution to this problem.

One advantage of TbD is that human factors are taken into account, by integrating the flexibility and adaptability of humans into the human-in-the-loop robotic systems [11]. For now, however, a number of problems needed to be addressed before its real applications in industry, one of which should be the development of approaches enabling robots to perform tasks in a human-like manner, in order to improve the robotic adaptability as stated above. Here, we use the term human-like referring to that robotic arms share the similarity of the adaptability of human limb muscle control strategies [12], [13]. This work aims to take one step towards this goal by developing a multimodal PbD system. The encoding of multimodal sensor signals has been verified effective in a number of task requirements, e.g., precision motion control [14]. Specifically, the multimoddal data considered in this work includes robotic endpoint states (i.e., position and velocity), EMG signal extracted from human arm, and force data collected from the force sensor mounted between the endpoint and the tool.

The presented approach is shown in Fig. 1. It basically consists of two parts: Learning and Reproduction. In the learning part, the collected data are used to estimate the model parameters. And in the reproduction part, the robot performs the same task as demonstrated with the learned knowledge. Specifically, our approach enables the robot to learn task information from human multimodal demonstration. The experiment result shows that the multimodal learning can achieve a better performance than using single modality when dealing a task with position and force constraints like pushing

some objects. The details of our approach will be present in Section III.

II. RELATED WORK

Generally, most work in the field of TbD has concentrated on the transfer of motion features from humans to robots through kinematics demonstration. This strategy has been successfully applied to several tasks where force constraints have small influences on the execution performance of the demonstrated tasks. When regarding *in-contact* tasks [15], however, stiffness/force regulation needs to be considered in addition to position constraints. Several papers have recently reported their methods on the regulation of stiffness/force in the process of human-robot skill transfer (see, e.g., [16]–[19]). Generally, like humans motor learning [20], variable impedance control is also needed for robots to satisfy both position and force constraints, in order for compliant adaptation to different task requirements.

Typically, the gains in the impedance controller are regulated by representing them with the use of a function approximator. The approximator is initialized with constant gains and then refined with reinforcement learning techniques [21]–[23]. It usually needs many trials to ultimately learn the proper stiffness profiles. In [15], [24], the stiffness matrix is estimated over the collected set of demonstrated force profiles, where the stiffness adaptation highly depends on the distribution of the force along relevant directions.

In this paper, we propose a more natural way for the realization of stiffness adaptation by estimating the human tutor's limb stiffness based on the EMG signals and then transferring the stiffness to the robot arm. The human arm endpoint stiffness can be traced online by using a computationally efficient Cartesian stiffness estimation model [25], [26]. The EMG-based impedance control strategy has been instigated and successfully applied to a number of robotic systems (see, e.g., [13], [27]). Here, we directly collect the EMG data from the human tutor's upper limb for stiffness estimation along with kinematics demonstration, without the need of a learning process of obtaining proper stiffness profiles.

For the encoding of the demonstration data, Dynamic Movement Primitive (DMP) is a widely used approach. In our previous work [28], [29], we developed a DMP framework for the representing of the motion and the stiffness simultaneously. However, DMP models each variable separately, without considering the correlation information between different variables. Instead, probabilistic algorithms such as Hidden Markov Model (HMM) can be used to represent the correlation by encoding a joint-probability density function over the demonstration data. In [30], a HMM-based approach is proposed with the combination of Gaussian Mixture Regression (GMR) to generate the control variables via regression. In [31], Hidden Semi-Markov Model (HSMM) is further used instead of the HMM model, in order to improve the robustness of the robotic system against external perturbations in temporal space. In [15], the HSMM-GMR model is further used to model motion as well as force data for in-contact tasks.

Inspired by the work [15], [30], [31], in this paper we further extend the HSMM model by adding another joint-probability density function for the modelling of the distribution between position and stiffness. This extended information is based on the fact that the demonstration profiles from human about force, velocity and stiffness, as well as their co-relation with the positions, are all crucial for the robot to learn. Therefore, such learned model is further integrated into a EMG-based variable impedance control strategy as a unified skill representation model. thus enabling to integrate EMG-based variable impedance control strategy into the unified skill representation model. GMR is as well used to generate the expected control variables, which are then properly mapped into an impedance controller.

III. METHODOLOGY

A. EMG-BASED STIFFNESS EXTRACTION

First, the raw EMG signals collected from the human tutor's arm are processed to extract an enveloping, which is used to reflect the co-activation level of the muscles. Generally, a moving average process and a low-pass filter are employed to obtain the enveloping. Based on the co-activation level, the human tutor's arm endpoint stiffness can be estimated by using a commonly-used perturbation procedure [27], during which several trials with various arm conditions are performed to identify the mapping between the position displacement of the human arm endpoint and the restoring force applied onto the endpoint. Once the endpoint stiffness matrix is determined, during demonstration the human arm endpoint stiffness can be obtained in a real time manner. Finally, the human endpoint stiffness needs to be mapped into the robot impedance controller in the joint space. In order to make the robot work functionally, the amplitudes of the stiffness profiles are restricted within a proper range of stiffness values. Here, we do not provide much description about this part, please see [13], [27] for more details.

B. HSMM-GMR MODEL DESCRIPTION

Considering a set of observations collected from the demonstrations, i.e., $\{x_m, \dot{x}_m, k_m, F_m\}_{m=1}^{M}$, where x and $\dot{x}$ represent the position and velocity of the robot endpoint, respectively; k the robot endpoint stiffness described above, and F the force collected from the force sensor mounted onto the robot endpoint.

First, HSMM is used to model the demonstration data. Then, GMR is used to generate the expected control variables based on the estimated parameters of the HSMM model.

1) DATA MODELLING WITH HSMM

The HSMM model is usually parametrized by:

$$\Theta = \{\{a_{i,j}\}_{j=1,j\neq i}^{K}, \pi_i, \mu_i^D, \Sigma_i^D, \boldsymbol{\mu}_i, \boldsymbol{\Sigma}_i\}_{i=1}^{K} \quad (1)$$

where K is the model states. π_i is the initial probability of the ith state. a_{ij} represents the transition probability from state j to i. μ_i^D and Σ_i^D are means and variances, respectively, modelling the K Gaussian parametric duration distributions.

$\boldsymbol{\mu}_i$ and $\boldsymbol{\Sigma}_i$ represent mean vectors and covariance matrices of the K joint observation probabilities, respectively.

The ith state duration probability density function is defined as

$$p_i^D(t) = \mathcal{N}(t; \mu_i^D, \Sigma_i^D) \tag{2}$$

with $t = 1, \ldots, t_{max}$, where t_{max} is the maximum allowed duration of a HSMM state which can be determined by

$$t_{max} = \gamma \frac{T_{max}}{K} \tag{3}$$

where T_{max} is the samples of these demonstrations. γ is a scaling factor that is usually set 2 such that state duration probability density function can be well modelled even if EM converges poorly [31].

The observation probability at each time step t for the ith state is defined by

$$p_i(z_t) = \mathcal{N}(z_t; \boldsymbol{\mu}_i, \boldsymbol{\Sigma}_i) \tag{4}$$

with ${}^1\boldsymbol{z}_t = [\boldsymbol{x}_t^T \ \dot{\boldsymbol{x}}_t^T]^T$, ${}^2\boldsymbol{z}_t = [\boldsymbol{x}_t^T \ \boldsymbol{k}^T]^T$ and ${}^3\boldsymbol{z}_t = [\boldsymbol{x}_t^T \ \boldsymbol{F}^T]^T$ are the concatenation of the observed variables at each time step t, corresponding to the three sets of observations, i.e., $\{x_m, \dot{x}_m\}_{m=1}^M$, $\{x_m, k_m\}_{m=1}^M$, and $\{x_m, F_m\}_{m=1}^M$, respectively.

For simplicity, then, the mean vector $\boldsymbol{\mu}_i$ and the covariance matrix $\boldsymbol{\Sigma}_i$ of each of these concatenations are separately represented as

$$\begin{cases} {}^1\boldsymbol{\mu}_i = \begin{bmatrix} \mu_i^x \\ \mu_i^{\dot{x}} \end{bmatrix} \\ {}^1\boldsymbol{\Sigma}_i = \begin{bmatrix} \Sigma_i^{xx} & \Sigma_i^{x\dot{x}} \\ \Sigma_i^{\dot{x}x} & \Sigma_i^{\dot{x}\dot{x}} \end{bmatrix} \end{cases} \tag{5}$$

and

$$\begin{cases} {}^2\boldsymbol{\mu}_i = \begin{bmatrix} \mu_i^x \\ \mu_i^k \end{bmatrix} \\ {}^2\boldsymbol{\Sigma}_i = \begin{bmatrix} \Sigma_i^{xx} & \Sigma_i^{xk} \\ \Sigma_i^{kx} & \Sigma_i^{kk} \end{bmatrix} \end{cases} \tag{6}$$

and

$$\begin{cases} {}^3\boldsymbol{\mu}_i = \begin{bmatrix} \mu_i^x \\ \mu_i^F \end{bmatrix} \\ {}^3\boldsymbol{\Sigma}_i = \begin{bmatrix} \Sigma_i^{xx} & \Sigma_i^{xF} \\ \Sigma_i^{Fx} & \Sigma_i^{FF} \end{bmatrix} \end{cases} \tag{7}$$

The three sets of $\{\mu_i, \Sigma_i\}$ are used to parametrize the joint Gaussian distributions $\mathcal{P}(x, \dot{x})$, $\mathcal{P}(x, k)$, and $\mathcal{P}(x, F)$, respectively. Namely, these three joint Guassian distributions are modelled in parallel (see Fig. 2). The parameters of the HSMM model, i.e., Θ are estimated based on the demonstration data.

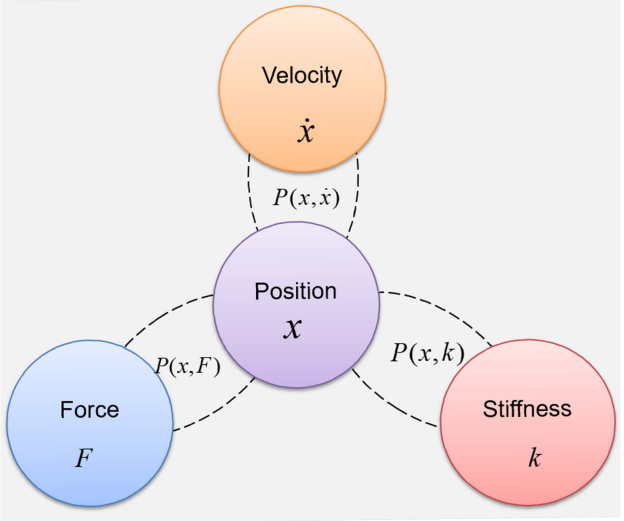

FIGURE 2. Graphical representation of the basic idea of the multimodal robotic learning strategy, in which three joint Gaussian distributions are used to encode the multimodal signals. The three HSMM models are trained separately in this work.

2) TASK REPRODUCTION WITH GMR

We compute the expected control variables with the GMR model. Their expectations are computed according to the current HSMM state given the reference position:

$$\dot{\boldsymbol{x}}_t^* = \sum_{i=1}^{K} h_{i,t}[\mu_i^{\dot{x}} + \Sigma_i^{\dot{x}x}(\Sigma_i^{xx})^{-1}(\boldsymbol{x}_t - \mu_i^x)] \tag{8}$$

$$\boldsymbol{k}^* = \sum_{i=1}^{K} h_{i,t}[\mu_i^k + \Sigma_i^{kx}(\Sigma_i^{xx})^{-1}(\boldsymbol{x}_t - \mu_i^x)] \tag{9}$$

$$\boldsymbol{F}_t^* = \sum_{i=1}^{K} h_{i,t}[\mu_i^F + \Sigma_i^{Fx}(\Sigma_i^{xx})^{-1}(\boldsymbol{x}_t - \mu_i^x)] \tag{10}$$

where $h_{i,t}$ represents the brief distribution of the Kth HSMM state. It should be noted that the model parameters $\{\mu_i, \Sigma_i, h_{i,t}\}$ should be different for each corresponding HSMM-GMM model since different modal data have been taken as input into the different models for training. Here, for simplicity they are written in the same format.

And $h_{i,t}$ are computed by

$$h_{i,t} = \mathcal{P}(s_t = i; z_{1:t}) = \frac{a_{i,t}}{\sum_{\kappa=1}^{K} a_{\kappa,t}} \tag{11}$$

The denotation $a_{i,t}$ represents the forward variable of the HSMM model and computed by

$$a_{i,t} = \sum_{j=1}^{K} \sum_{d=1}^{\min(t_{max}, t-1)} a_{j,t-d} a_{j,i} p_i^D(d) \prod_{s=t-d+1}^{t} \mathcal{N}(x_s; \mu_i^x, \Sigma_i^{xx}) \tag{12}$$

with initiation in each sate:

$$a_{i,1} = \pi_i \mathcal{N}(\boldsymbol{x}_1; \mu_i^x, \Sigma_i^{xx}) \tag{13}$$

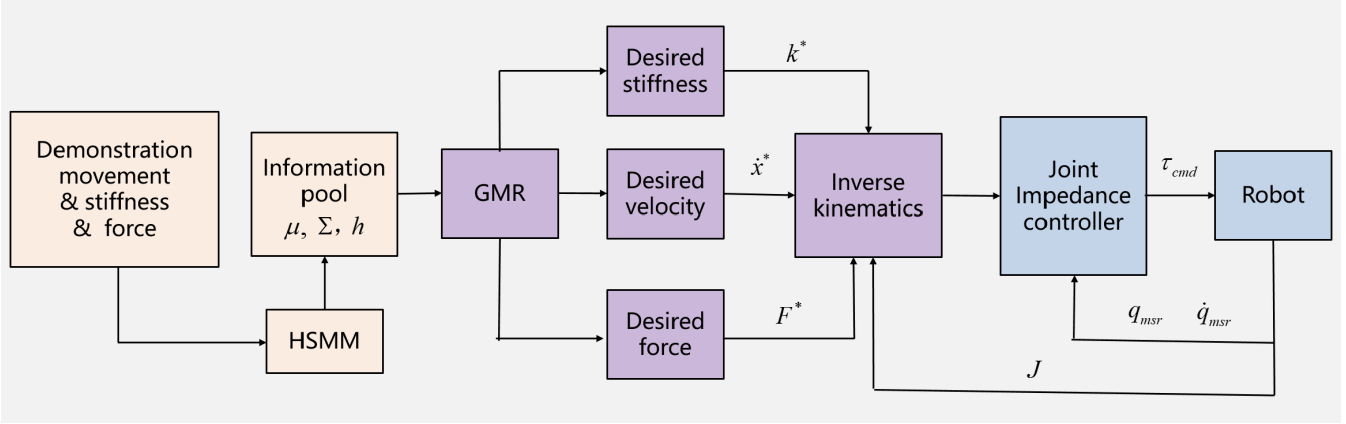

FIGURE 3. The HSMM-GMR skill learning diagram. The HSMM model parameters μ, Σ and h are offline estimated to form the information pool. During the reproduction phase, the desired stiffness, velocity and force are computed based on the GMR model. The computed variables are then fit into the joint impedance controller through inverse Kinematics. Finally, the computed torques are sent to the robot joints which are enabled under the torque control mode.

where $\boldsymbol{x}_1$ represents the starting point of the robot endpoint position trajectory. Please see [30] and [31] for more details of the HSMM-GMR model.

To summarize, once the reference positions $\boldsymbol{x}_t$ and the estimated parameters of the HSMM's states are obtained, the expected velocities, stiffness profiles and force can be calculated by 8, 9 and 10, respectively.

C. IMPEDANCE CONTROLLER

In this work, the robot arm is controlled under the torque control mode with an impedance controller in joint space. Here, we use a commonly used controller, the formation of which consists of four parts:

$$\boldsymbol{\tau}_{cmd} = \boldsymbol{K}_j(\boldsymbol{q}^* - \boldsymbol{q}_{msr}) + \boldsymbol{D}(\dot{\boldsymbol{q}}^* - \dot{\boldsymbol{q}}_{msr}) + \boldsymbol{J}^T\boldsymbol{F}^* + \boldsymbol{\tau}_{dyn}(q, \dot{q}, \ddot{q}) \quad (14)$$

where $\boldsymbol{q}^*$ and $\boldsymbol{q}_{msr}$ are the desired and the measured joint angles during the phase of task reproduction; $\dot{\boldsymbol{q}}^*$ and $\dot{\boldsymbol{q}}_{msr}$ are the desired and the measured joint velocities. $\boldsymbol{K}_j$ and $\boldsymbol{D}$ are the joint stiffness and damping coefficients, respectively. $\boldsymbol{J}$ is the Jacobian matrix of the robot arm. $\boldsymbol{F}^*$ is the desired endpoint force obtained from 10. $\boldsymbol{\tau}_{dyn}(q, \dot{q}, \ddot{q})$ represents the dynamical model of the arm compensating for the forces, i.e., the gravity, the inertia and the Coriolis forces. The dynamical term can be usually identified by several techniques such as adaptive control, and assumed known in our work when the robot is controlled under the torque control mode. $\boldsymbol{\tau}_{cmd}$ is the generated torque applied to the robot joint. The whole control diagram is shown in Fig. 3.

The measured joint angles $\boldsymbol{q}_{msr}$ and velocities $\dot{\boldsymbol{q}}_{msr}$ are directly obtained from the interface provided by the robot manufacturer. The desired joint angles $\boldsymbol{q}^*$ are computed through inverse kinematics based on the desired endpoint position. The desired joint velocities $\dot{\boldsymbol{q}}^*$ are computed by:

$$\dot{\boldsymbol{q}}^* = \boldsymbol{J}^+\dot{\boldsymbol{x}}^* \quad (15)$$

where $\boldsymbol{J}^+$ represents the pseudo-inverse Jacobian matrix, and it is defined by:

$$\boldsymbol{J}^+ = \boldsymbol{J}^T \cdot inv(\boldsymbol{J}\boldsymbol{J}^T + 0.001\boldsymbol{I}) \quad (16)$$

with one unit matrix $\boldsymbol{I}$.

The joint stiffness matrix $\boldsymbol{K}_j$ is computed in accordance with the robot endpoint stiffness:

$$\boldsymbol{K}_j = \boldsymbol{J}^T diag(k_i)\boldsymbol{J} \quad (17)$$

Finally, the joint damping matrix $\boldsymbol{D}$ can be determined by

$$\boldsymbol{D} = diag(d_i) \quad (18)$$

with

$$d_i = \sigma_i\sqrt{k_i} \quad (19)$$

where σ_i are predefined constant coefficients.

IV. EXPERIMENTAL VALIDATION

A. DESCRIPTION

We test our approach on the Baxter robot. The robot arm can be controlled under the torque model with impedance adaptation. An EMG device (MYO armband) is used for collecting the EMG signals from the human tutor's arm during the demonstration phase. A six-axis force sensor (ATI Mini-45) is mounted between the endpoint of one of the robot arms and the tool for collecting the force signals.

The experimental system for the human demonstration is shown in Fig. 4. During demonstration, the EMG signals are collected with the MYO armband and then sent through Blutooth to a computer for processing. The interaction force signals are collected and amplified by the collection board, then sent to the same computer. The processed stiffness and force data are then sent to the host computer through UPD protocol, and then simultaneously recorded along with the robot sate variables. During the reproduction phase, only the host computer is needed and the generated joint torque commands are directly sent to the robotic joint actuators.

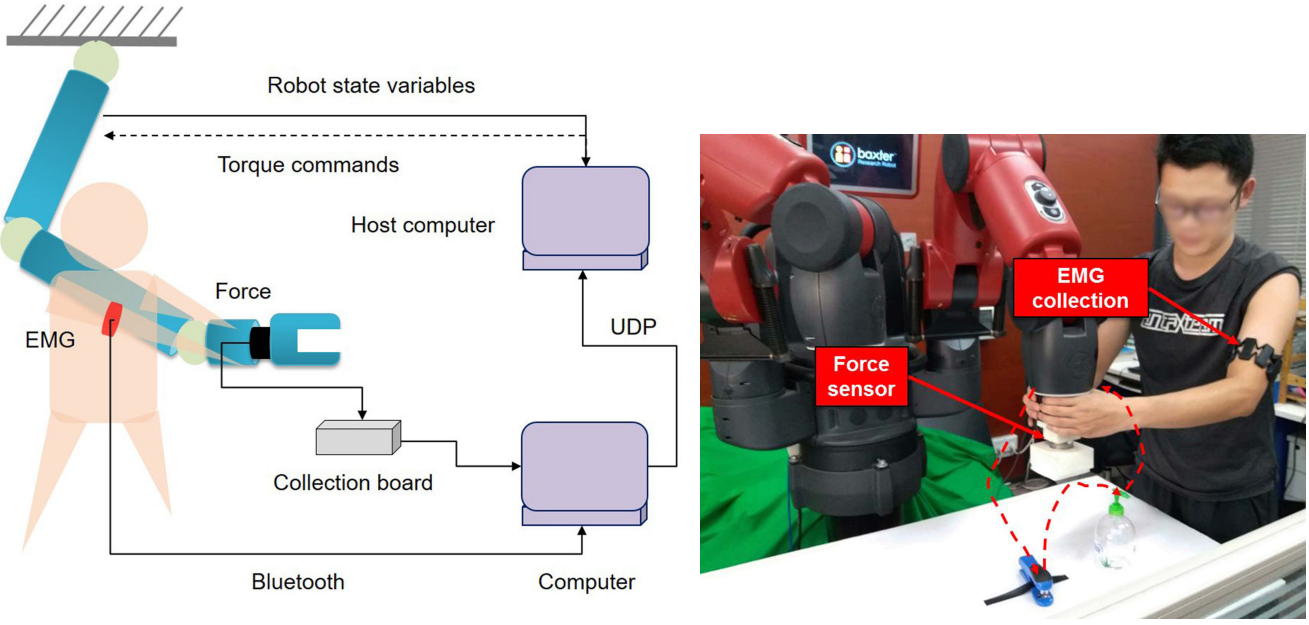

FIGURE 4. (a) Graphical reinterpretation of the experimental system. During demonstration, multimodal signals (the robot state variables, human arm EMG signals and the interaction force between the robot and the environment) are simultaneously collected. All the needed variables are recorded at the same sampling rate on the host computer. (b) The experimental setup during the multimodal demonstration phase. The robot endpoint movement trajectories, the EMG signals and the force data are recorded simultaneously during skill demonstration. Note that the first object (stapler) is fixed onto the desk, while the second object (bottle) is placed on the desk without any constraint.

The experimental procedure follows three basic phases including:

i) *Demonstration*: Firstly, the human tutor demonstrates the robot to perform a pushing-pushing tasks for several times (see Fig. 4), under the built-in kinematics teaching mode provided by the robot manufacturer. During demonstration, the robot endpoint posture is recorded, plus the force data and the human arm endpoint stiffness profiles. Note that the human tutor's hands hold on the robot endpoint during the pushing-pushing process.

ii) *Model learning*: Then, the demonstration data (i.e., the set $\{x_i, \dot{x}_i, k, F_i\}, i = 1, 2, 3$) are used to fit the HSMM model for the estimation of the model parameters. The main code we used is the implementation freely provided by Dr. S. Calinon's group[1] [32], [33]. The orientations are not considered in this work and therefore fixed during the experiment.

iii) *Reproduction*: Finally, the robot reproduces the task under the variable impedance controller with the control variables (position, stiffness and force) generated by the GMR model.

B. EXPERIMENTAL SETTINGS

There are total 15 sets of demonstration data collected for the pushing-pushing task. The sample rates for the EMG signals and the force are set as 100 Hz and 200 Hz, respectively. During the reproduction phase, the orientation is fixed as $[\pi, 0, 0]rad$, and the stiffness parameters in orientation are set as $[20, 20, 20]\frac{Nm}{rad}$.

[1]https://gitlab.idiap.ch/rli/pbdlib-matlab/

TABLE 1. The settings for the three test conditions.

Con.	EMG/Stiffness	Force	Motion traj.
Condition 1	√	√	√
Condition 2	√	×	√
Condition 3	×	√	√

The tasks reproduction is conducted under the following three conditions:

Condition 1: with EMG and force. The robot reproduces the task with both variable impedance control and force feedforward. In this case, the learned stiffness profiles are used as variable gains in the impedance controller.

Condition 2: with EMG, without force. The robot performs the task under the variable impedance controller with the learned control variables but without the force term, which means that the robot is controlled under a force-free mode.

Condition 3: with force, without EMG. The robot reproduces the task with force feedforward and impedance controller but with constant gains. The stiffness parameter in z axis is fixed as a constant value.

In summary, as shown in Table 1, the first condition is set to validate the proposed control strategy. The second test condition is to show the performance of the control strategy with only EMG signals, while the third condition is to show that with only force but without the utilization of the EMG data.

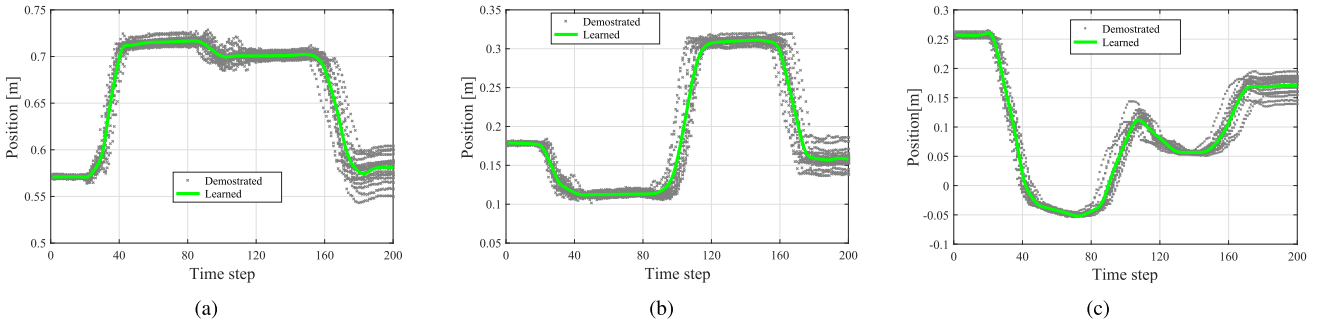

FIGURE 5. The position trajectories in the robot end-effector x, y and z axis respectively. The positions (green lines) are generated based the demonstration ones (gray dots).

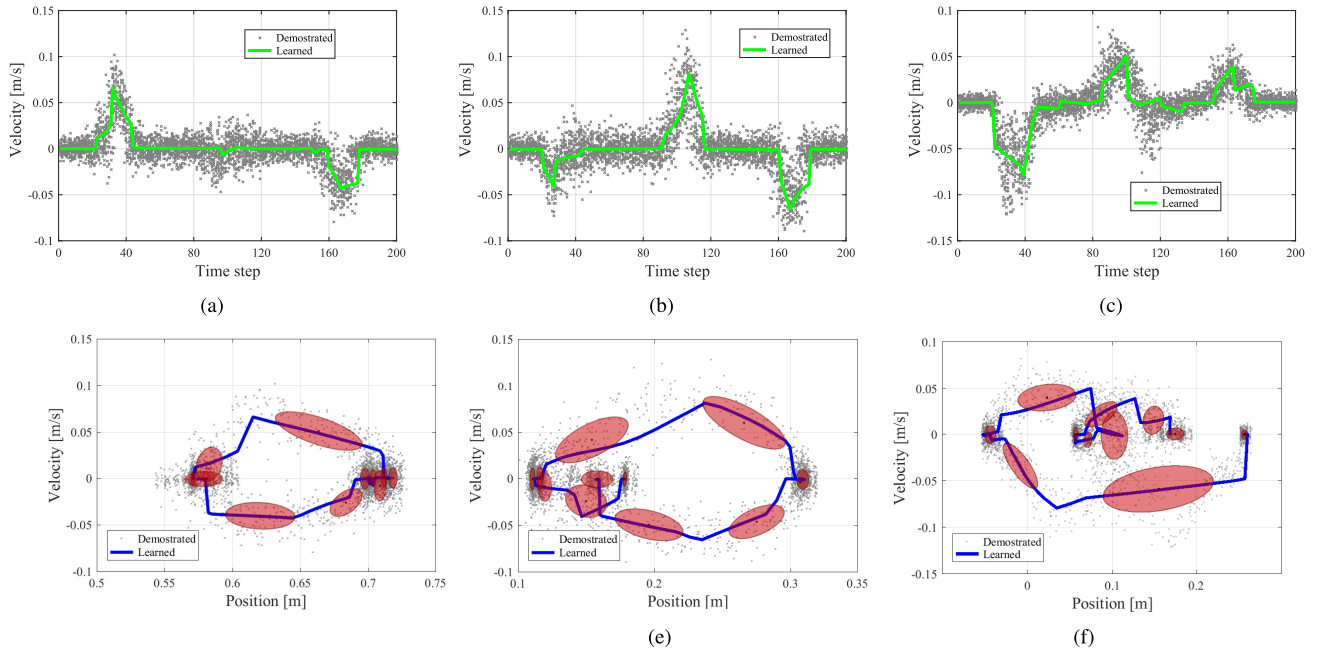

FIGURE 6. (a)-(c) show the velocity trajectories in x, y and z axis respectively. The velocities (green lines) are computed by GMR model based the demonstration ones (gray dots). (d)-(f) are the learned velocity trajectories with respect to the position trajectories with the fitted Gaussian models.

C. RESULTS AND DISCUSSION

The learned position trajectories and the computed velocity trajectories by GMR model with respect to the demonstration data are shown in Fig. 5 and Fig. 6, respectively. And the learned velocity profiles with respect to the position trajectories are shown in Fig. 6(d)-(f). The computed stiffness in z axis with respect to the demonstration ones is shown in Fig. 7. A typical example of the measured position and force (z axis) trajectories with respect to the demonstrated ones are shown in Fig. 8. The visual inspection shows that the robot achieves the best performance under Condition 1, compared with the other two conditions.

We perform the reproductions for several times under each of these test conditions. Under condition 1, the robot is able to smoothly execute the task, and no obvious variance is observed under this condition. The robot fails to push down the two objects under Condition 2 (see the red lines in Fig. 8(b) and (c)), this can be explained by the low force applied onto the robotic endpoint. Under test Condition 3, the task is successfully performed by the robotic arm even obtaining a bit better performance of position tracking. This is because that the robot manipulator has a better capability of dealing with external perturbations when controlled with high impedance.

Under constant stiffness control mode, however, the robot is not able to reproduce the adaptability of the force to the task situation as demonstrated and as the learned one. Large variance in force is observed under condition 3 (see the black line in Fig. 8 as an example). Note that the second object (i.e., the bottle) is not fixed in our experiment. In this case, the rigid robot arm trends to push it away when contacting with the bottle, resulting in the sudden changes of the force profile [see Fig. 8(b)]. It suggests that condition 3 may easily cause unstable interactions between the robot and its environment.

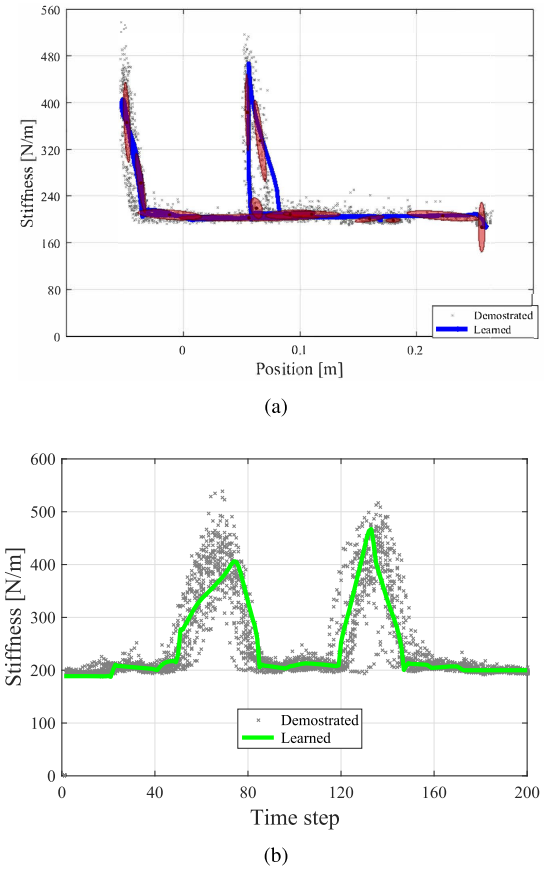

FIGURE 7. The stiffness profiles with respect to (a) position and (b) time step in z axis. The red oval areas represent the fitted Gaussian models.

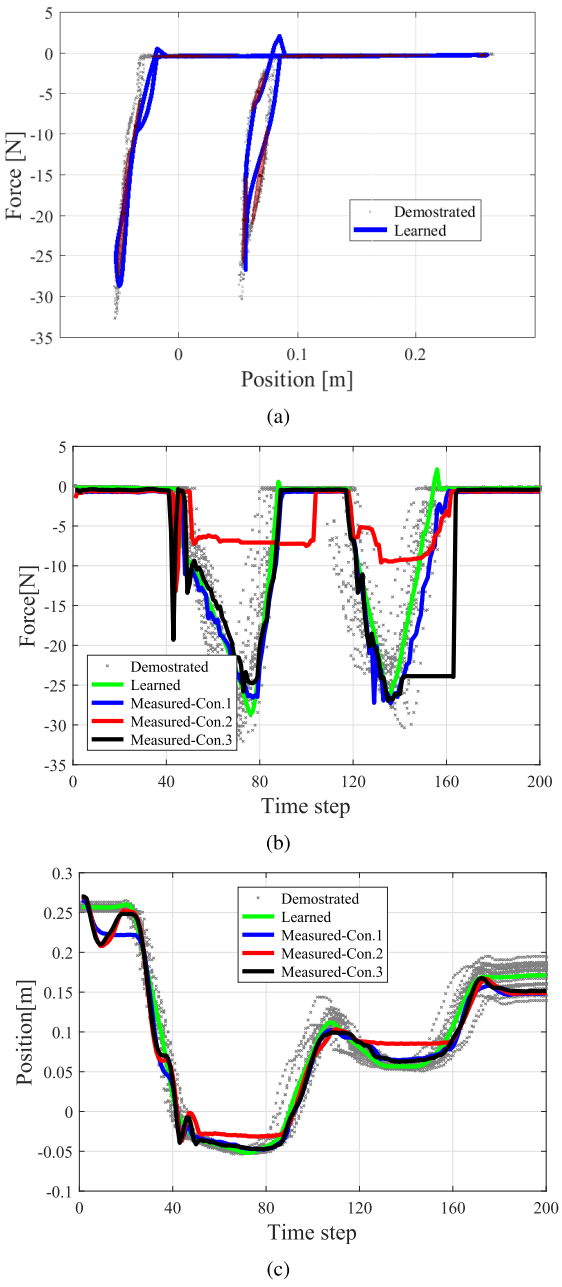

FIGURE 8. The force profiles with respect to (a) position and (b) time step in z axis. The red areas in (a) are the fitted Gaussian models. (c) represents the measured potion trajectories of the robotic endpoint in z axis during the task reproduction phase. The blue, red and black lines correspond to the first, second and the third experimental conditions, respectively. The sudden changes (black line) are due to the unstable interaction under the third test condition.

The force remaining constant from 140 to 160 time steps may be explained by that there was not enough time for the force sensor to response when the unstable interaction happened. It should be easy to understand that the robot arm with constant high stiffness keeps robust to the external perturbation despite of the unstable interaction, and thus the position of the robotic endpoint in z direction can almost follow the desired one [see Fig. 8(c) 120-160 time steps].

There is a small mismatch in time coordination between the stiffness and the force, which may be explained by the non-synchronously collecting of the EMG force signals during demonstration, and by separately training of the stiffness and the force data. Note that the measured force profiles are not only determined by the learned stiffness but also the learned force (see the controller, i.e., Eq. 14). Therefore, even in the stable interaction (the fist pushing) the observed robot behaviour should be different. We can also see that from 8(b) (about the 40th time step) the constant impedance interaction (condition 2) might cause large contact force, which is basically consistent with the experimental findings in [27].

When humans interact with external environments, we often trend to adapt our arm impedance rather than using a rigid manner [34]. These results show that our method enable robots to learn the features of movement trajectories, stiffness and force profiles from human demonstration. By encoding multiple sensing signals to extract the correlations between position and the other variables with the combination of HSMM and GMR, our method can generate decent control commands from the demonstration data even the dynamics of these trajectories are complex.

The stiffness and force profiles have demonstrated the features as expected: keep low when getting close to the

targets and then increase to push the objects. It should be noted that the adaptation features of the stiffness and force are directly extracted from human demonstration. Multiple information data (movement, stiffness and force) are included in the proposed teaching-by-demonstration system. In this way, a more complete skill transfer process can be achieved than only considering one or two signals.

Compared with previous studies (e.g., [15]), our model does not directly encode the ''strong'' correlation between stiffness and force by separately training the three HSMM models, leaving room for the individually optimizing of impedance and feedforward force, as suggested by the findings in human arm motor learning [20], [34].

One drawback of our approach is that sometimes the models are different to train when the demonstrated profiles have a large variance (see Fig. 6 and Fig. 7(b) 40-80 time steps). It may potentially require more demonstration data or larger number of Gaussian models to learn a perfect profile, which would increase the computational cost.

V. CONCLUSION

In this paper, we propose a teaching-by-demonstration approach considering multiple sensor signals for robots to learn skill features from humans, including movement trajectories, stiffness profiles and force data. The stiffness profiles are obtained by the estimation of the human tutor's arm impedance based on the collection of the EMG signals, and the force data are collected from the force sensor rigidly mounted onto the robotic endpoint. These three types of signals are integrated together by encoding the three Gaussian distributions, i.e., between position and velocity, stiffness and force, using the HSMM model. Then, GMR is used to generate the control variables to fit the robotic impedance controller, based on the learned parameters of HSMM. Finally, we demonstrate the validity of the proposed method by a real-word experiment based on the Baxter robot. The experiment suggests compared with the constant stiffness control with only force-sensing involved, the proposed multimodal approach can enable the robot to both successfully and stably perform the pushing task. Our method has potential applications in a number of tasks that need both stiffness adaptation and force control.

Future work will be focused on the fusion of the multiple signals in a higher level by integrating some cross-modal learning techniques (see, e.g., [35]) into the proposed teaching-by-demonstration system, in order to improve the robotic capabilities of learning high-level action strategies. Furthermore, optimization techniques may be utilized to online refine the stiffness and the force profiles once they are learned from the demonstration data.

REFERENCES

[1] F. Chen, K. Sekiyama, F. Cannella, and T. Fukuda, ''Optimal subtask allocation for human and robot collaboration within hybrid assembly system,'' *IEEE Trans. Autom. Sci. Eng.*, vol. 11, no. 4, pp. 1065–1075, Oct. 2014.

[2] J. Duan, Y. Ou, J. Hu, Z. Wang, S. Jin, and C. Xu, ''Fast and stable learning of dynamical systems based on extreme learning machine,'' *IEEE Trans. Syst., Man, Cybern., Syst.*, vol. 49, no. 6, pp. 1175–1185, Jun. 2019.

[3] Y. Xu, C. Yang, J. Zhong, N. Wang, and L. Zhao, ''Robot teaching by teleoperation based on visual interaction and extreme learning machine,'' *Neurocomputing*, vol. 275, pp. 2093–2103, Jan. 2018.

[4] Y. Yang, Y. Li, C. Fermuller, and Y. Aloimonos, ''Robot learning manipulation action plans by 'Watching' unconstrained videos from the world wide Web,'' in *Proc. 29th AAAI Conf. Artif. Intell.*, 2015, pp. 3686–3692.

[5] A. Billard, S. Calinon, R. Dillmann, and S. Schaal, ''Robot programming by demonstration,'' in *Springer Handbook of Robotics*. Berlin, Germany: Springer, 2008, pp. 1371–1394.

[6] A. G. Billard, S. Calinon, and R. Dillmann, ''Learning from humans,'' in *Springer Handbook of Robotics*. Cham, Switzerland: Springer, 2016, pp. 1995–2014.

[7] Z. Zhu and H. Hu, ''Robot learning from demonstration in robotic assembly: A survey,'' *Robotics*, vol. 7, no. 2, p. 17, 2018.

[8] C. Zeng, C. Yang, Z. Chen, and S.-L. Dai, ''Robot learning human stiffness regulation for hybrid manufacture,'' *Assembly Autom.*, vol. 38, no. 5, pp. 539–547, 2018.

[9] L. Rozo, S. Calinon, D. G. Caldwell, P. Jiménez, and C. Torras, ''Learning physical collaborative robot behaviors from human demonstrations,'' *IEEE Trans. Robot.*, vol. 32, no. 3, pp. 513–527, Jun. 2016.

[10] Y. Li, G. Ganesh, N. Jarrassé, S. Haddadin, A. Albu-Schaeffer, and E. Burdet, ''Force, impedance, and trajectory learning for contact tooling and haptic identification,'' *IEEE Trans. Robot.*, vol. 34, no. 5, pp. 1170–1182, Oct. 2018.

[11] L. Peternel, T. Petrič, and J. Babič, ''Human-in-the-loop approach for teaching robot assembly tasks using impedance control interface,'' in *Proc. IEEE Int. Conf. Robot. Autom. (ICRA)*, May 2015, pp. 1497–1502.

[12] C. Yang, G. Ganesh, S. Haddadin, S. Parusel, A. Albu-Schäffer, and E. Burdet, ''Human-like adaptation of force and impedance in stable and unstable interactions,'' *IEEE Trans. Robot.*, vol. 27, no. 5, pp. 918–930, Oct. 2011.

[13] C. Yang, C. Zeng, P. Liang, Z. Li, R. Li, and C.-Y. Su, ''Interface design of a physical human–robot interaction system for human impedance adaptive skill transfer,'' *IEEE Trans. Autom. Sci. Eng.*, vol. 15, no. 1, pp. 329–340, Jan. 2018.

[14] R. Yang, P. Er, Z. Wang, and K. Tan, ''An RBF neural network approach towards precision motion system with selective sensor fusion,'' *Neurocomputing*, vol. 199, pp. 31–39, Jul. 2016.

[15] M. Racca, J. Pajarinen, A. Montebelli, and V. Kyrki, ''Learning in-contact control strategies from demonstration,'' in *Proc. IEEE/RSJ Int. Conf. Intell. Robots Syst. (IROS)*, Oct. 2016, pp. 688–695.

[16] W. He, Y. Chen, and Z. Yin, ''Adaptive neural network control of an uncertain robot with full-state constraints,'' *IEEE Trans. Cybern.*, vol. 46, no. 3, pp. 620–629, Apr. 2016.

[17] F. Steinmetz, A. Montebelli, and V. Kyrki, ''Simultaneous kinesthetic teaching of positional and force requirements for sequential in-contact tasks,'' in *Proc. IEEE-RAS 15th Int. Conf. Humanoid Robots*, Nov. 2015, pp. 202–209.

[18] W. He and Y. Dong, ''Adaptive fuzzy neural network control for a constrained robot using impedance learning,'' *IEEE Trans. Neural Netw. Learn. Syst.*, vol. 29, no. 4, pp. 1174–1186, 2018.

[19] B. Nemec, N. Likar, A. Gams, and A. Ude, ''Human robot cooperation with compliance adaptation along the motion trajectory,'' *Auto. Robots*, vol. 42, no. 5, pp. 1023–1035, 2018.

[20] E. Burdet, R. Osu, D. W. Franklin, T. E. Milner, and M. Kawato, ''The central nervous system stabilizes unstable dynamics by learning optimal impedance,'' *Nature*, vol. 414, no. 6862, pp. 446–449, Nov. 2001.

[21] F. Stulp, J. Buchli, A. Ellmer, M. Mistry, E. A. Theodorou, and S. Schaal, ''Model-free reinforcement learning of impedance control in stochastic environments,'' *IEEE Trans. Auton. Mental Develop.*, vol. 4, no. 4, pp. 330–341, Dec. 2012.

[22] J. Buchli, F. Stulp, E. A. Theodorou, and S. Schaal, ''Learning variable impedance control,'' *Int. J. Robot. Res.*, vol. 30, no. 7, pp. 820–833, Apr. 2011.

[23] Z. Li, T. Zhao, F. Chen, Y. Hu, C.-Y. Su, and T. Fukuda, ''Reinforcement learning of manipulation and grasping using dynamical movement primitives for a humanoidlike mobile manipulator,'' *IEEE/ASME Trans. Mechatronics*, vol. 23, no. 1, pp. 121–131, Feb. 2018.

[24] L. D. Rozo, S. Calinon, D. Caldwell, P. Jiménez, and C. Torras, ''Learning collaborative impedance-based robot behaviors,'' in *Proc. AAAI Conf. Artif. Intell.*, 2013, pp. 1422–1428.

[25] A. Ajoudani, C. Fang, N. G. Tsagarakis, and A. Bicchi, "A reduced-complexity description of arm endpoint stiffness with applications to teleimpedance control," in *Proc. IEEE/RSJ Int. Conf. Intell. Robots Syst. (IROS)*, Sep. 2015, pp. 1017–1023.
[26] C. Fang, A. Ajoudani, A. Bicchi, and N. G. Tsagarakis, "Online model based estimation of complete joint stiffness of human arm," *IEEE Robot. Autom. Lett.*, vol. 3, no. 1, pp. 84–91, Jan. 2018.
[27] A. Ajoudani, N. Tsagarakis, and A. Bicchi, "Tele-impedance: Teleoperation with impedance regulation using a body–machine interface," *Int. J. Robot. Res.*, vol. 31, no. 13, pp. 1642–1656, 2012.
[28] C. Yang, C. Zeng, C. Fang, W. He, and Z. Li, "A DMPs-based framework for robot learning and generalization of humanlike variable impedance skills," *IEEE/ASME Trans. Mechatronics*, vol. 23, no. 3, pp. 1193–1203, Jun. 2018.
[29] C. Yang, C. Zeng, Y. Cong, N. Wang, and M. Wang, "A learning framework of adaptive manipulative skills from human to robot," *IEEE Trans. Ind. Informat.*, vol. 15, no. 2, pp. 1153–1161, Feb. 2019.
[30] S. Calinon, F. D'Halluin, E. L. Sauser, A. G. Billard, and D. G. Caldwell, "Learning and reproduction of gestures by imitation," *IEEE Robot. Autom. Mag.*, vol. 17, no. 2, pp. 44–54, Jun. 2010.
[31] S. Calinon, A. Pistillo, and D. G. Caldwell, "Encoding the time and space constraints of a task in explicit-duration hidden Markov model," in *Proc. IEEE/RSJ Int. Conf. Intell. Robots Syst.*, Sep. 2011, pp. 3413–3418.
[32] S. Calinon, "A tutorial on task-parameterized movement learning and retrieval," *Intell. Service Robot.*, vol. 9, no. 1, pp. 1–29, 2016.
[33] L. Rozo, J. Silvério, S. Calinon, and D. G. Caldwell, "Learning controllers for reactive and proactive behaviors in human-robot collaboration," *Frontiers Robot. AI*, vol. 3, no. 30, pp. 1–11, Jun. 2016.
[34] E. Burdet, G. Ganesh, C. Yang, and A. Albu-Schäffer, "Interaction force, impedance and trajectory adaptation: By humans, for robots," in *Experimental Robotics*. Berlin, Germany: Springer, 2014, pp. 331–345.
[35] M. A. Lee, Y. Zhu, K. Srinivasan, P. Shah, S. Savarese, L. Fei-Fei, A. Garg, and J. Bohg, "Making sense of vision and touch: Self-supervised learning of multimodal representations for contact-rich tasks," 2018, *arXiv:1810.10191*. [Online]. Available: https://arxiv.org/abs/1810.10191

CHAO ZENG (S'18) received the M.S. degree in precision instrument and mechanics from Shanghai University, Shanghai, China, in 2016. He is currently pursuing the Ph.D. degree with the College of Automation Science and Engineering, South China University of Technology, Guangzhou, China. From October 2018 to October 2019, he is a Visiting Ph.D. Student with the TAMS Group, University of Hamburg, Hamburg, Germany. His current research interests include human–robot interaction, programming by demonstration, and human robot skill transfer.

CHENGUANG YANG (M'10–SM'16) received the Ph.D. degree in control engineering from the National University of Singapore, Singapore, in 2010.

He performed as a Postdoctoral Research in human robotics with the Imperial College London, London, U.K., from 2009 to 2010. He is currently a Professor of robotics with the Bristol Robotics Laboratory, Bristol, U.K. His research interests include human–robot interaction and intelligent system design. He was a recipient of a EU Marie Curie International Incoming Fellowship, a U.K. EPSRC UKRI Innovation Fellowship, and the Best Paper Award of the IEEE TRANSACTIONS ON ROBOTICS, as well as over ten conference best paper awards.

JUNPEI ZHONG received the B.Eng. degree from the South China University of Technology, in 2006, the M.Phil. degree from Hong Kong Polytechnic University, in 2010, and the Ph.D. degree (Hons.) from the University of Hamburg, in 2015. He was a Researcher with the National Institute of Advanced Industrial Science and Technology (AIST), Waseda University, and Plymouth University. He was also involved with three European projects and one Japanese project. He is currently an Independent Research Fellow and a Lecturer of computational intelligence and cognitive robotics with Nottingham Trent University, U.K. He has published more than 30 journals and conference papers. His research interests include machine learning, robotics, and assistive technologies. He was a recipient of the three-year Marie-Curie Early Career Studentship, in 2010. He acted as the Guest Editor of *Complexity*, the IEEE TRANSACTIONS ON COGNITIVE AND DEVELOPMENTAL SYSTEMS, and the *Journal of Ambient Intelligence and Humanized Computing*. He is also the Chair of the IEEE Symposium of Domestic Robotics, in 2019.

JIANWEI ZHANG (M'91) received the B.S. and M.S. degrees from the Department of Computer Science, Tsinghua University, Beijing, China, in 1986 and 1989, respectively, and the Ph.D. degree from the Department of Computer Science, Institute of Real-Time Computer Systems and Robotics, University of Karlsruhe, Karlsruhe, Germany, in 1994.

He is currently a Professor and the Head of the TAMS Group, University of Hamburg, Hamburg, Germany. He has published more than 200 journals and conference papers, technical reports, four book chapters, and two research monographs. His research interests include multimodal perception, robot learning, and mobile service robots. He was a recipient of several awards, including the IEEE ROMAN and the IEEE AIM Best Paper Awards.